BMC Complementary Medicine and Therapies

RESEARCH

Open Access

Gallic acid rescues uranyl acetate induced-hepatic dysfunction in rats by its antioxidant and cytoprotective potentials

Ibtisam M. H. Elmileegy[1], Hanan S. A. Waly[2], Alshaimaa A. I. Alghriany[3], Nasser S. Abou Khalil[1,4*], Sara M. M. Mahmoud[5] and Eman A. Negm[5]

Abstract

Background The liver was identified as a primary target organ for the chemo-radiological effects of uranyl acetate (UA). Although the anti-oxidant and anti-apoptotic properties of gallic acid (GA) make it a promising phytochemical to resist its hazards, there is no available data in this area of research.

Methods To address this issue, eighteen rats were randomly and equally divided into three groups. One group was received carboxymethyl cellulose (vehicle of GA) and kept as a control. The UA group was injected intraperitoneally with UA at a single dose of 5 mg/kg body weight. The third group (GA + UA group) was treated with GA orally at a dose of 100 mg/kg body weight for 14 days before UA exposure. UA was injected on the 15th day of the experiment in either the UA group or the GA + UA group. The biochemical, histological, and immunohistochemical findings in the GA + UA group were compared to both control and UA groups.

Results The results showed that UA exposure led to a range of adverse effects. These included elevated plasma levels of aspartate aminotransferase, lactate dehydrogenase, total protein, globulin, glucose, total cholesterol, triglycerides, low-density lipoprotein cholesterol, and very-low-density lipoprotein and decreased plasma levels of high-density lipoprotein cholesterol. The exposure also disrupted the redox balance, evident through decreased plasma total antioxidant capacity and hepatic nitric oxide, superoxide dismutase, reduced glutathione, glutathione-S-transferase, glutathione reductase, and glutathione peroxidase and increased hepatic oxidized glutathione and malondialdehyde. Plasma levels of albumin and alanine aminotransferase did not significantly change in all groups. Histopathological analysis revealed damage to liver tissue, characterized by deteriorations in tissue structure, excessive collagen accumulation, and depletion of glycogen. Furthermore, UA exposure up-regulated the immuno-expression of cleaved caspase-3 and down-regulated the immuno-expression of nuclear factor-erythroid-2-related factor 2 in hepatic tissues, indicating an induction of apoptosis and oxidative stress response. However, the pre-treatment with GA proved to be effective in mitigating these negative effects induced by UA exposure, except for the disturbances in the lipid profile.

*Correspondence:
Nasser S. Abou Khalil
nasser82@aun.edu.eg

Full list of author information is available at the end of the article

Conclusions The study suggests that GA has the potential to act as a protective agent against the adverse effects of UA exposure on the liver. Its ability to restore redox balance and inhibit apoptosis makes it a promising candidate for countering the harmful effects of chemo-radiological agents such as UA.

Keywords Uranyl acetate, Gallic acid, Liver, Physiology, Nrf2, Apoptosis

Background

The enduring presence of depleted uranium (DU) in bio-ecological systems, its diverse entry routes, magnification through the food chain, and the compounded effects of both metallic and radiation toxicities [1, 2] establish it as a prominent environmental pollutant. Among vulnerable organs to DU-related issues, the liver stands out due to its role as a center for xenobiotic accumulation and metabolism [3]. The intoxication with uranyl acetate (UA) led to a breakdown of the protective antioxidant shield in the liver, primarily driven by reduced nuclear translocation of nuclear factor-erythroid-2-related factor 2 (Nrf2). UA-induced molecular changes resulting in apoptosis within the liver involved the activation of caspase-3, elevation of Bcl-2/Bax ratio, release of cytochrome c from mitochondria, and decrease in ATP levels, all collectively promoting cellular death [3–5]. The attack by free radicals and initiation of the apoptotic pathway lead to degenerative and necrotic modifications in hepatocytes, subsequently releasing liver metabolic enzymes into the bloodstream [4]. Thus, employing bioactive compounds with antioxidant and cytoprotective properties could potentially counteract UA-induced hepatotoxicity. Although sequestering agents have been widely used to counteract UA radiotoxicity, they often yield unsatisfactory outcomes due to their nonspecific affinity, limited efficacy, insufficient clinical trials, and potential to induce acid-base imbalance and renal toxicity [1, 6, 7].

These challenges are driving a new wave of research focused on natural biological approaches to mitigate chemo-radiological risks posed by UA. Our laboratory demonstrated the effectiveness of thymoquinone and N-acetylcysteine against UA-induced testicular damage in rats, primarily through their anti-apoptotic and cytoprotective mechanisms rather than their antioxidant properties [8]. Substantial evidence from animal models and cell cultures supports the protective potential of gallic acid (GA) on irradiated livers. Supplementation of mice exposed to gamma rays with GA prevented the depletion of antioxidant defenses and excessive lipid peroxidation in the liver [9]. However, the impact of GA on hepatic metabolic enzyme activity remains unstudied. Ferk et al. [10] reported that GA intervention alleviated gamma radiation-induced genotoxic damage and preneoplastic foci in rats. They attributed these effects to the antioxidant potency of GA, believed to stem from redox-related transcription regulator up-regulation, without solid molecular evidence. Other studies using a mouse model of dimethylnitrosamine-induced hepatotoxicity revealed that GA increased Nf2 transcript levels, which subsequently bound to DNA sequences to activate redox stabilizers' expression [11]. Nonetheless, whether GA can mitigate UA-induced hepatic dysfunction remains uncertain. Hence, this study aims to address this gap by evaluating potential changes in plasma metabolic enzymes, liver redox homeostasis, histological features, as well as caspase-3 and Nrf2 immuno-expression in Wistar rats.

Methods

Drugs and chemicals

UA dihydrate (purity ≥ 98% and molecular weight 424.15 g/mol) was purchased from Sigma-Aldrich Company (St. Louis, MO, USA). GA (purity ≥ 99%) was obtained from Sd Fine Chem. Limited Company, India. Carboxymethyl cellulose (CMC) 98% CAS: 9005-64-5 was obtained from Alpha Global Search Company, New York, USA.

Experimental animals

A total of 18 adult male Wistar rats were used for this study. The rats were purchased from the Egyptian Company for Production of Vaccines, Sera, and Drugs, Egypt, and housed under natural light/dark cycles, at a temperature of 20–25 °C, and relative humidity of 55.0 ± 5.0%. They were provided with commercial pelleted feed and water *ad libitum*.

Experimental design

After a one-week acclimatization period, the rats were randomly divided into three groups, each consisting of six animals. The control group received carboxymethyl cellulose (CMC); the vehicle of GA. The second group (UA group) received an intraperitoneal injection of UA at a single dose of 5 mg/kg body weight [4]. The third group (GA + UA group) was orally administered GA using a stomach tube at a dose of 100 mg/kg body weight [12] dissolved in 1% CMC for 14 days prior to UA exposure. UA was injected on the 15th day of the experiment in either the UA group or the GA + UA group.

Collection and preparation of samples

At the end of the experimental period, blood samples were collected from the retro-orbital sinus after overnight fasting. Plasma was separated by centrifugation at 3000 rpm for 10 min and stored at -20 °C for subsequent biochemical analyses. Rats were euthanized by cervical

dislocation under anesthesia induced by intraperitoneal injection of sodium thiopental. Half of the liver was promptly excised, homogenized in 1 ml of 0.1 M phosphate buffer (pH 7.4), and centrifuged at 10,000 rpm for 15 min using IKA Yellow line DI homogenizer (18 Disperser, Germany) to give 10% w/v homogenate. The homogenates were centrifuged at 10.000 rpm for 15 min, and the resulting supernatants were frozen at -20 °C for measurement of oxidant/antioxidant parameters. The other half of liver was fixed in 10% neutral buffered formalin for histopathological evaluation. The experimental procedure was represented in Fig. 1.

Biochemical measurements

Plasma alanine aminotransferase (ALT) (Catalog number: 264001), aspartate aminotransferase (AST) (Catalog number: 260001), albumin level (Catalog number: 211001), total protein (Catalog number: 310001), glucose (Catalog number: 250001), total cholesterol (TC) (Catalog number: 230002), triglyceride (TG) (Catalog number: 314002), and high-density lipoprotein cholesterol (HDL-C) (Catalog number: 266001) were assessed according to the manufacturer's instructions using commercial kits provided by Egyptian Company for Biotechnology Company, Egypt. Plasma low-density lipoprotein cholesterol

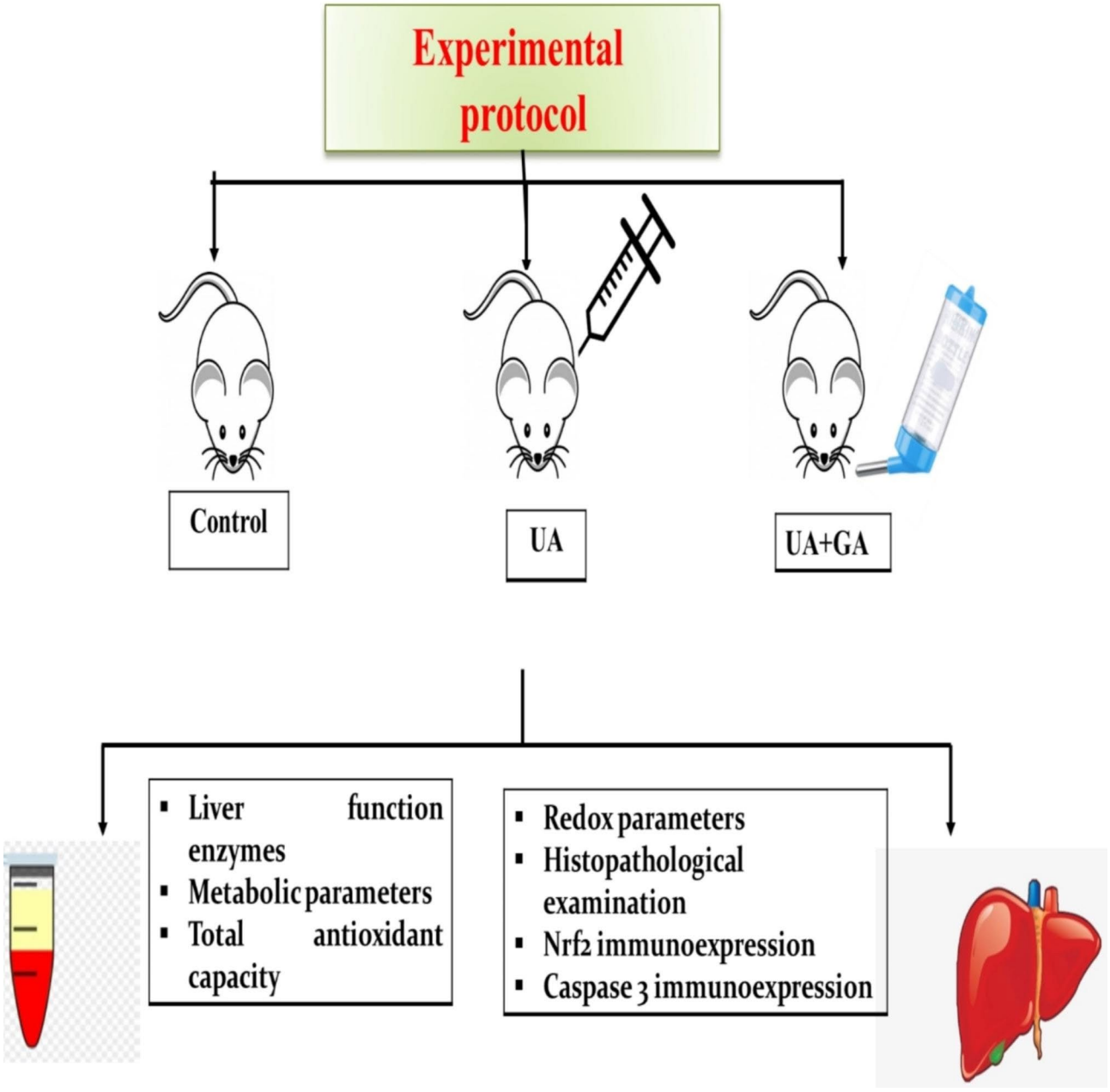

Fig. 1 Graphical representation of the experimental procedure. UA: uranyl acetate; GA: gallic acid; Nrf2: nuclear factor-erythroid-2-related factor 2

(LDL-C) was determined using the Friedewald formula: LDL-C=TC − HDL-C − [TG/5] [13]. Plasma very-low-density lipoprotein (VLDL) was calculated according to [14].

Total globulins were calculated by subtracting the obtained albumin level from the obtained total proteins level [15]. Plasma lactate dehydrogenase (LDH) activity was measured by a kinetic method using a commercial kit (Catalog number: 2940, Stabino Laboratory Company, Texas, Egypt). The levels of malondialdehyde (MDA) were measured by thiobarbituric acid reaction according to the procedure of Ohkawa et al. [16]. Nitric oxide (NO) was measured as nitrite concentration using the method of Ding et al. [17]. Total antioxidant capacity (TAC) was measured using a calorimetric kit (Catalog number: TA2513, Biodiagnostic, Giza, Egypt). Superoxide dismutase (SOD) activity was determined based on its inhibition of epinephrine autoxidation [18]. Reduced glutathione (GSH) content was estimated using the method of Beutler et al. [19]. Oxidized glutathione (GSSG) levels were measured by the enzymatic recycling method described by Tietze [20]. Glutathione peroxidase (GPx) activity was determined by measuring the decrease in GSH content after incubating the sample in the presence of hydrogen peroxide and sodium azide [21]. Glutathione reductase (GR) activity was assayed by following the oxidation of NADPH by GSSG [19]. Glutathione-S-transferase (GST) activity was determined from the rate of increase in conjugate formation between reduced glutathione and 1-chloro-2,4-dinitrobenzene [22]. All the measured oxidant/antioxidant parameters were corrected with total protein levels in the hepatic homogenate, and were measured using a spectrophotometer (S1200, Unico, USA).

Histological and histochemical examinations

Liver sections were fixed in 10% neutral buffered formalin, processed using the paraffin-embedding technique, and then sectioned for staining. Hematoxylin and eosin stain was used for general histological examination [23], Picrosirius red stain for collagen identification [24], and Periodic acid Schiff (PAS) for glycogen content [23]. Examination and photography were carried out utilizing a digital camera (Toup Tek ToupView, Copyrightc 2019, Version:x86, Compatible: Windows XP/Vista/7/8/10, China), ImageJ software, and a computer connected to a light microscope (Olympus CX31, Japan).

Immunohistochemistry of cleaved caspase-3 and Nrf2

Formalin-fixed liver tissues were put in 10% neutral buffered (pH 7.2). Paraffin-embedded tissues were sectioned, cleared, and rehydrated in a grade of ethanol solutions (100% −70%) and rinsed in water. Extraction of antigens was done by boiling the slides in 1 mM ethylenediaminetetraacetic acid for 10 min, and emerging sections in 3% H_2O_2 for 10 min. Each section was put in a blocking solution at room temperature for one hour. The primary cleaved caspase-3 antibody (1:1000) (Novus Biologicals, LLC, USA) and anti-Nrf2 antibody (1:500) (GeneTex, Inc. North America) were then added for 24 h, followed by the secondary antibodies (1:5000) for two hours. After establishing the reaction with 3,3′-diaminobenzidine for 2–3 min, the sections were stained with hematoxylin for 2–5 min [25].

Statistical analysis

Data were represented as mean±standard error of the mean (SEM). The results were analyzed by one-way analysis of variance (ANOVA) followed by Duncan post-test using SPSS program version 16 (SPSS Inc., Chicago, USA). Differences of $p<0.05$ were considered to be statistically significant.

Results

Effects of GA on liver function parameters in UA-intoxicated rats

Exposure to UA resulted in a significant increase in AST, LDH, total protein, globulin, and glucose, with no significant change in ALT and albumin. Supplementation with GA before UA intoxication normalized the AST, LDH, and glucose, although total protein and globulin became higher than the control group. There was no significant change when comparing ALT and albumin in the UA group with the GA+UA group (Table 1). UA-challenged rats exhibited hypercholesterolemia and hypertriglyceridemia compared to the control group. A significant reduction in HDL-C and a significant elevation in LDL-C and VLDL were found in the UA-intoxicated rats. GA intervention failed to significantly improve the studied lipid profile compared to the UA group (Table 2).

Effects of GA on plasma total antioxidant capacity and hepatic redox balance in UA-intoxicated rats

A significant reduction was observed in plasma TAC in the UA group compared to the control group. Liver tissues from UA-exposed rats demonstrated a significant increase in MDA and GSSG and a significant decrease in NO, SOD, GSH, GST, GR, and GPx. GA supplementation effectively returned plasma TAC and hepatic MDA, SOD, GSH, and GST to the control levels. The hepatic GR and GPx in the UA+GA group were significantly improved compared to the UA group, but they were still significantly lower than the UA group. The hepatic NO in the GA+UA group was significantly higher than the control group. The hepatic GSSG was significantly reduced in the GA+UA group but still significantly higher than the control group (Table 3).

Table 1 The effect of gallic acid on the plasma liver function parameters following uranyl acetate-induced liver dysfunction in rats

Parameters/Groups	Control	UA	GA + UA	*P* value
Plasma ALT activity (U/L)	9.007 ± 0.389	8.604 ± 0.222	9.063 ± 0.206	0.474
Plasma AST activity (U/L)	0.141 ± 0.011	0.222 ± 0.020$^{\#}$	0.146 ± 0.017$^{\&}$	0.0150
Plasma LDH activity (U/L)	24.645 ± 3.170	227.880 ± 76.316$^{\#}$	65.410 ± 9.306$^{\&}$	0.011
Plasma albumin level (g/dl)	2.836 ± 0.106	2.939 ± 0.061	2.954 ± 0.188	0.785
Plasma globulin level (g/dl)	1.790 ± 0.159	3.850 ± 0.524$^{\#}$	4.422 ± 0.813$^{\Omega}$	0.004
Plasma TP level (g/dl)	4.693 ± 0.205	6.375 ± 0.613$^{\#}$	7.536 ± 0.800$^{\Omega}$	0.009
Plasma glucose level (mg/dl)	87.594 ± 15.807	193.892 ± 20.750$^{\#}$	116.462 ± 22.152$^{\&}$	0.003

UA: uranyl acetate; GA: gallic acid; AST: aspartate aminotransferase; ALT: Alanine aminotransferase; LDH: lactate dehydrogenase; TP: Total protein

Results are expressed as mean ± SEM of 6 rats per group (One-way ANOVA followed by Duncan post-test)

#= significant difference between UA and the control groups

&= significant difference between GA + UA and UA groups

Ω = significant difference between GA + UA and the control groups

Table 2 Effect of gallic acid on the plasma lipid profile following uranyl acetate-induced liver dysfunction in rats

Parameters/Groups	Control	UA	GA + UA	*P* value
Plasma TC level (mmol/l)	65.812 ± 3.897	92.943 ± 6.280$^{\#}$	97.534 ± 5.432$^{\Omega}$	0.001
Plasma TG level (mg/dl)	54.456 ± 2.904	85.737 ± 8.115$^{\#}$	99.373 ± 6.262$^{\Omega}$	0.001
Plasma HDL-C level (mg/dl)	41.167 ± 2.212	24.700 ± 1.327$^{\#}$	22.642 ± 1.217$^{\Omega}$	0.000
Plasma LDL-C level (mg/dl)	24.453 ± 1.314	36.600 ± 1.621$^{\#}$	40.755 ± 2.190$^{\Omega}$	0.000
Plasma VLDL level (mg/dl)	13.162 ± 0.779	18.643 ± 1.089$^{\#}$	19.475 ± 0.794$^{\Omega}$	0.000

UA: uranyl acetate; GA: gallic acid; TC: total cholesterol; TG: triglycerides; HDL-C: high-density lipoprotein cholesterol; LDL-C: low-density lipoprotein cholesterol; VLDL: very-low-density lipoprotein

Results are expressed as mean ± SEM of 6 rats per group (One-way ANOVA followed by Duncan post-test)

#= significant difference between UA and the control groups

Ω = significant difference between GA + UA and the control groups

Table 3 Effect of gallic acid on oxidant/antioxidant parameters following uranyl acetate-induced liver dysfunction in rats

Parameters/Groups	Control	UA	GA + UA	*P* value
Liver MDA level (nmol/mg protein)	3.649 ± 0.454	5.082 ± 0.558$^{\#}$	2.820 ± 0.413$^{\&}$	0.015
Liver NO level (nmol/mg protein)	96.138 ± 8.952	68.085 ± 6.149$^{\#}$	149.783 ± 11.535$^{\&\Omega}$	0.000
Plasma TAC (nmol/ml)	0.236 ± 0.043	0.069 ± 0.007$^{\#}$	0.192 ± 0.032$^{\&}$	0.005
Liver SOD activity (nmol/mg protein)	20.483 ± 1.332	7.077 ± 1.691$^{\#}$	19.230 ± 1.878$^{\&}$	0.001
Liver GSH level (nmol/mg protein)	15.385 ± 0.614	13.010 ± 0.363$^{\#}$	15.412 ± 0.587$^{\&}$	0.004
Liver GSSG level (nmol/mg protein)	0.372 ± 0.010	0.595 ± 0.017$^{\#}$	0.446 ± 0.013$^{\&\Omega}$	0.000
Liver GST level (μmol CDNB-GSH conjugate formed/min/mg protein)	62.969 ± 2.226	57.244 ± 2.023$^{\#}$	40.071 ± 1.416$^{\&}$	0.000
Liver GR activity (nmol of GSSG utilized/min/mg protein)	16.289 ± 0.842	8.144 ± 0.421$^{\#}$	13.031 ± 0.674$^{\&\Omega}$	0.000
Liver GPx activity (nmol of GSH oxidized/min/mg protein)	254.577 ± 5.732	178.204 ± 4.012$^{\#}$	229.119 ± 5.158$^{\&\Omega}$	0.000

UA: uranyl acetate; GA: gallic acid; MDA: malondialdehyde; NO: nitric oxide; TAC: total antioxidant capacity; SOD: superoxide dismutase; GSH: reduced glutathione; GSSG: oxidized glutathione; GST: glutathione-S-transferase; CDNB: 1-chloro-2,4-dinitrobenzene; GR: glutathione reductase; GPx: glutathione peroxidase

Results are expressed as the mean ± SEM of 6 rats per group (One-way ANOVA followed by Duncan post-test)

#= significant difference between UA and the control groups

&= significant difference between GA + UA and the UA groups

Ω = significant difference between GA + UA and the control groups

The effects of GA on the histological features of the liver of UA-intoxicated rats

Hematoxylin and Eosin staining of liver tissue from the control group revealed normal structure (Fig. 2a,b). The hepatocytes radiated in cords from the central vein. Blood sinusoids were located in between these cords. The hepatocytes contained one or two rounded vesicular nuclei and granulated cytoplasm. The portal area included the hepatic artery, portal vein, and bile ductule (Fig. 2b). UA exposure led to degenerated hepatocytes characterized by irregular nuclei and vacuolated cytoplasm. Fibrotic areas with cellular infiltration and extravasated blood cells were observed (Fig. 2c,d,e). GA supplementation prior to UA exposure resulted in nearly normal hepatocytes, with minimal fibrosis and cellular infiltration (Fig. 3a,b). Histopathological scoring confirmed the significant increase in degenerative parameters (vacuolated cytoplasm, irregular nuclei, karyolysis,

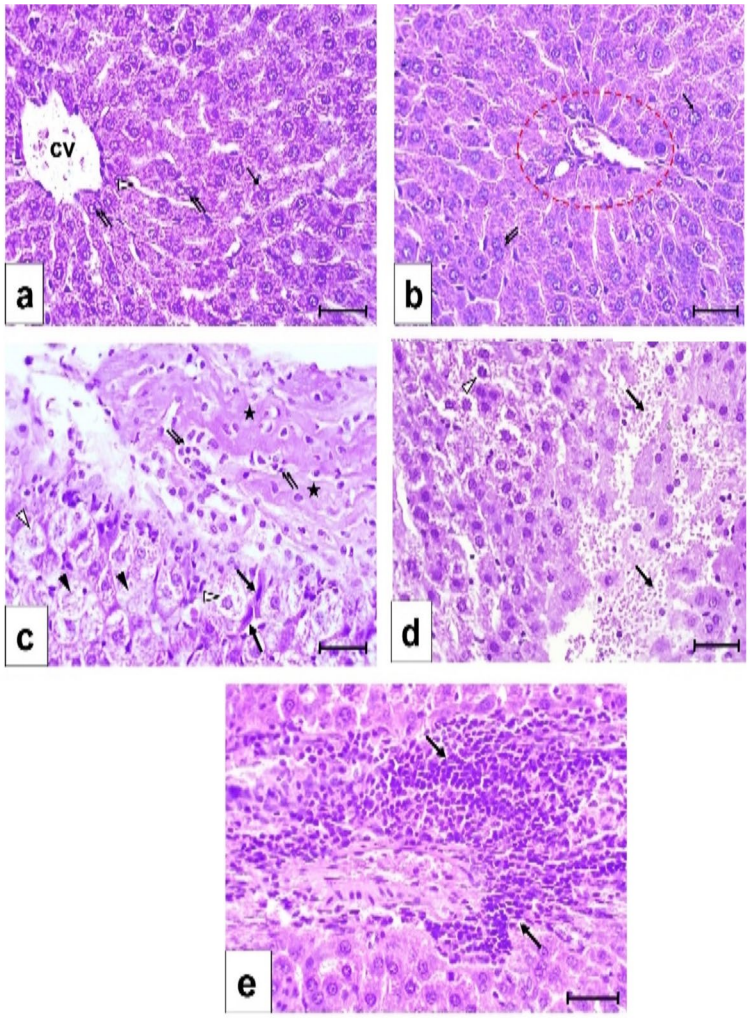

Fig. 2 Photomicrographs in the liver sections stained by H&E, bars = 50 μm (**a**) In control group showing a central vein (cv) from which mono- (↑) and binucleated (↑↑) hepatocytes are radiating in cords. The hepatocytes are with rounded vesicular nuclei and granular cytoplasm. Blood sinusoids are between the hepatic cords (Δ). (**b**) In control group showing a portal area (red circle). Mono- (↑) and binucleated (↑↑) hepatocytes are with rounded vesicular nuclei and granular cytoplasm. (**c**) In UA group showing massive fibrotic area (asterisk) enclosing connective tissue cells (↑↑). Hepatocytes are with pale vacuolated cytoplasm and irregular nuclei (Δ). Features of Karyolysis observed in some hepatocytes (▲). Some oval cells with dense flat nuclei noticed between hepatocytes (↑). (**d**) In UA group showing extravasated blood cells in between hepatocytes (↑). Some hepatocytes are with vacuolated cytoplasm and dense nuclei (Δ). (**e**) In UA group showing massive cellular infiltration (↑) around the portal area

hemorrhage, and cellular infiltration) in the UA group, while the GA + UA group exhibited insignificant changes compared to the control group (Fig. 3c).

The effects of GA on the collagen deposition and glycogen content in the liver of UA-intoxicated rats

Examination of collagen fibers by Picrosirius red stain in the control group showed a tiny amount around the central vein (Fig. 4a). Huge amount of collagen fibers was observed in the UA group, evidenced by the red color (Fig. 4b). A significant increase in the percentage of collagen area in the UA group was found compared to the control group (Fig. 4d). GA supplementation mitigated collagen deposition, resembling the control group (Fig. 4c). The percentage of the area of collagen amount in the different experimental groups was represented in Fig. 4d.

Glycogen content examination by PAS stain in the control group showed a great amount of glycogen content (Fig. 5a). Noticeable depletion in the glycogen content in most of the hepatocytes was observed in the UA group (Fig. 5b). GA supplementation restored glycogen content to levels similar to the control group (Fig. 5c). The percentage of the area of glycogen amount in the different experimental groups was represented in Fig. 5d.

The effects of GA on the immunohistochemistry of cleaved caspase-3 in the liver of UA-intoxicated rats

Immunohistochemical analysis of cleaved caspase-3 revealed a negative immunoreaction in the control group

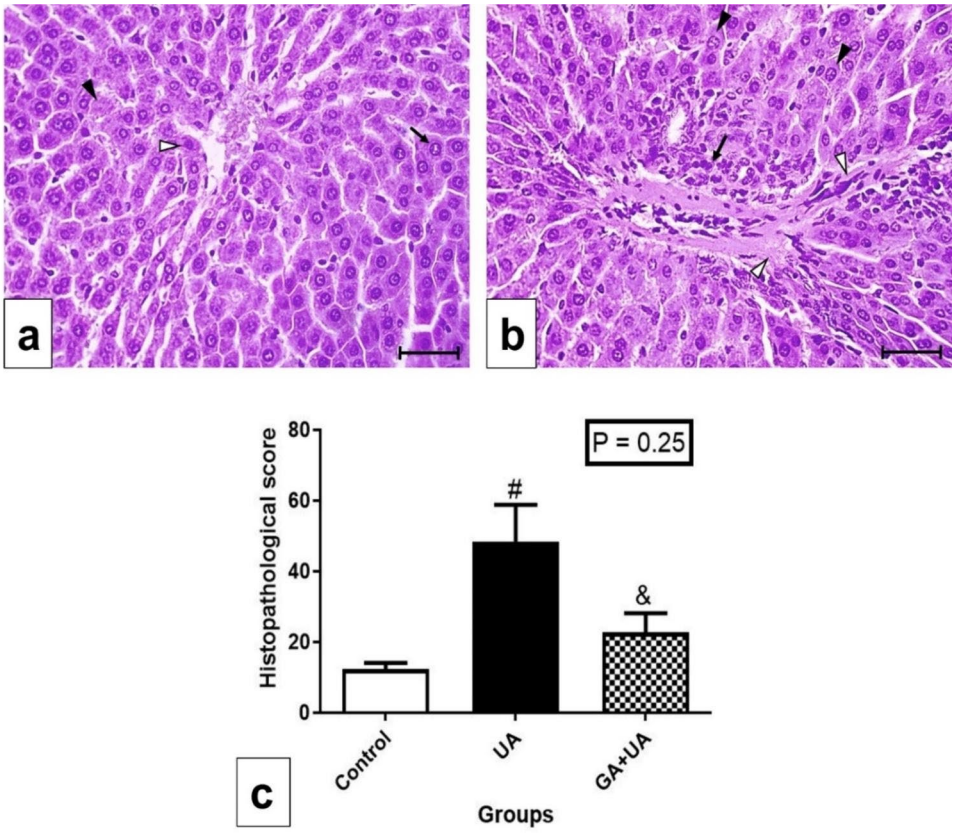

Fig. 3 Photomicrographs in the liver sections of GA + UA group stained by H&E, bars = 50 µm (a&b). (**a**) Showing nearly normal appearance of hepatocytes with rounded vesicular nuclei (↑). Few cells are with condensed nuclei (Δ) and the others showing Karyolysis (▲). (**b**) Showing cellular infiltration around the portal area (↑), and appearance of some fibers (Δ). The majority of hepatocytes are nearly normal (▲). (**d**) Liver histopathological score for all the experimental groups. Results are expressed as mean ± SEM of 3 rats per group (One-way ANOVA followed by Duncan post-test). # significant difference between UA and the control groups. & significant difference between GA + UA and UA groups

(Fig. 6a), contrasting the highly positive immunoreaction observed in the UA group (Fig. 6b). GA supplementation showed mostly negative immunoreaction, with minimal positive staining (Fig. 6c). The area of cleaved caspase-3 protein expression significantly increased in the UA group compared to the control group, while the GA group exhibited insignificant changes compared to the control group (Fig. 6d).

The effects of GA on the immunohistochemistry of Nrf2 in the liver of UA-intoxicated rats

Positive immunoreaction of Nrf2 was observed in the control group (Fig. 7a), while UA-exposed rats exhibited negative immunoreaction (Fig. 7b). GA supplementation resulted in positive immunoreaction similar to the control group (Fig. 7c). The area of Nrf2 protein expression significantly decreased in the UA group compared to the control group, with GA supplementation increased it to a level resembling that of the control group (Fig. 7d).

Discussion

The significant increase in plasma AST and LDH activities mirrors observations from a previous study [4]. In our experimental model, the oxidative burden triggered by UA led to hepatocyte cytolysis, causing the release of cytosolic enzymes into the bloodstream. The elevation in AST activity can be linked to increased production of Krebs cycle intermediates, contributing to fueling gluconeogenesis to meet cellular metabolic demands while maintaining antioxidative capacities to counteract redox imbalances [26]. The increased LDH activity is associated with lactic acidosis, which is implicated in apoptosis through opening the mitochondrial permeability transition pore and inducing cytosolic Ca^{2+} bursts that activate caspases [27]. Conversely, GA effectively normalized plasma AST and LDH activities, consistent with findings in paraquat-induced hepatotoxic rats [28]. The hepatoprotective mechanisms of GA involve hindering the access of oxygen-derived species to the lipid bilayer, reversing oxidative/nitrosative-mediated membrane disruptions, and stabilizing tight junctions and epithelial barriers [29–31].

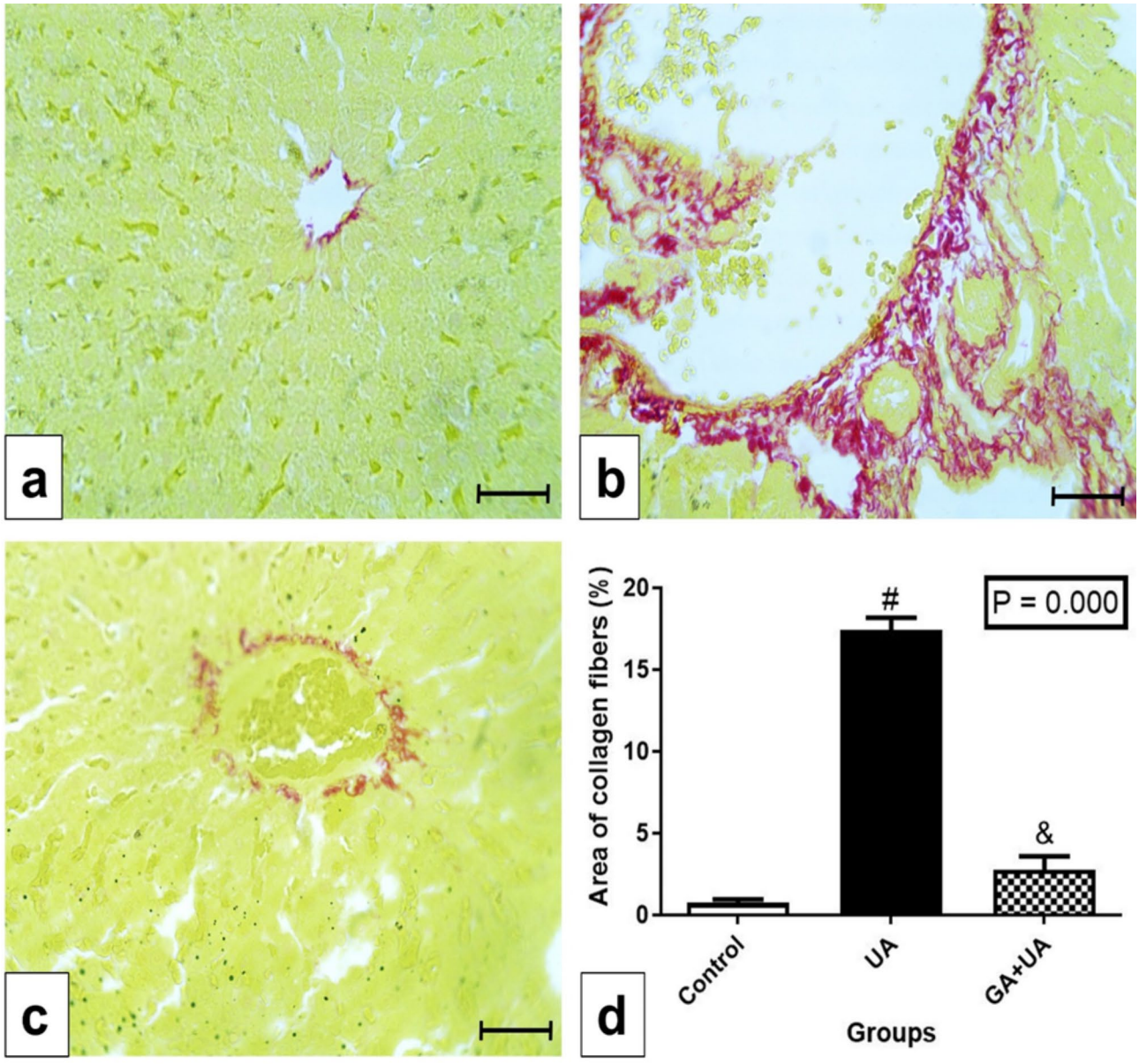

Fig. 4 Collagen fibers examination in the experimental groups. (**a**-**c**) photomicrographs of liver sections stained by Picrosirius red stain, bar = 50 µm. (**a**) In control group, showing tiny amount of collagen fibers around the central vein. (**b**) In UA group, showing huge amount of collagen fibers represented by the red color. (**c**) In GA + UA group, showing few amounts of collagen fibers nearly as those of control group. (**d**) Percentage of area of collagen fibers in the different experimental groups. Results are expressed as mean ± SEM of 3 rats per group (One-way ANOVA followed by Duncan post-test). # significant difference between UA and the control groups. & significant difference between GA + UA and UA groups

The UA-associated hyperglobulinemia in our experimental irradiated rats aligns with increased serum immunoglobulin levels observed in orally supplemented mice [32]. This suggests enhanced B cell differentiation to boost specific immunity against xenobiotic contamination or potential impairment in the ability of the liver to clear immunoglobulins from circulation [33, 34]. As part of a compensatory response to reactive damaging molecules, accelerated protein generation supports the biosynthesis of antioxidants and cytoprotective agents [35]. The hyperproteinemia observed in the UA group contradicts findings by Zimmerman and colleagues [36], who reported no significant change in total protein. However, it could serve as a symptomatic marker of hepatic dysfunction [37]. Hyperproteinemia may instigate generation of reactive free radicals and activation of programmed cell death through the endoplasmic reticulum-calcium ion signaling pathway [38] following UA exposure. It was hypothesized that the increase in albumin and ALT by hepatocellular injury was masked by

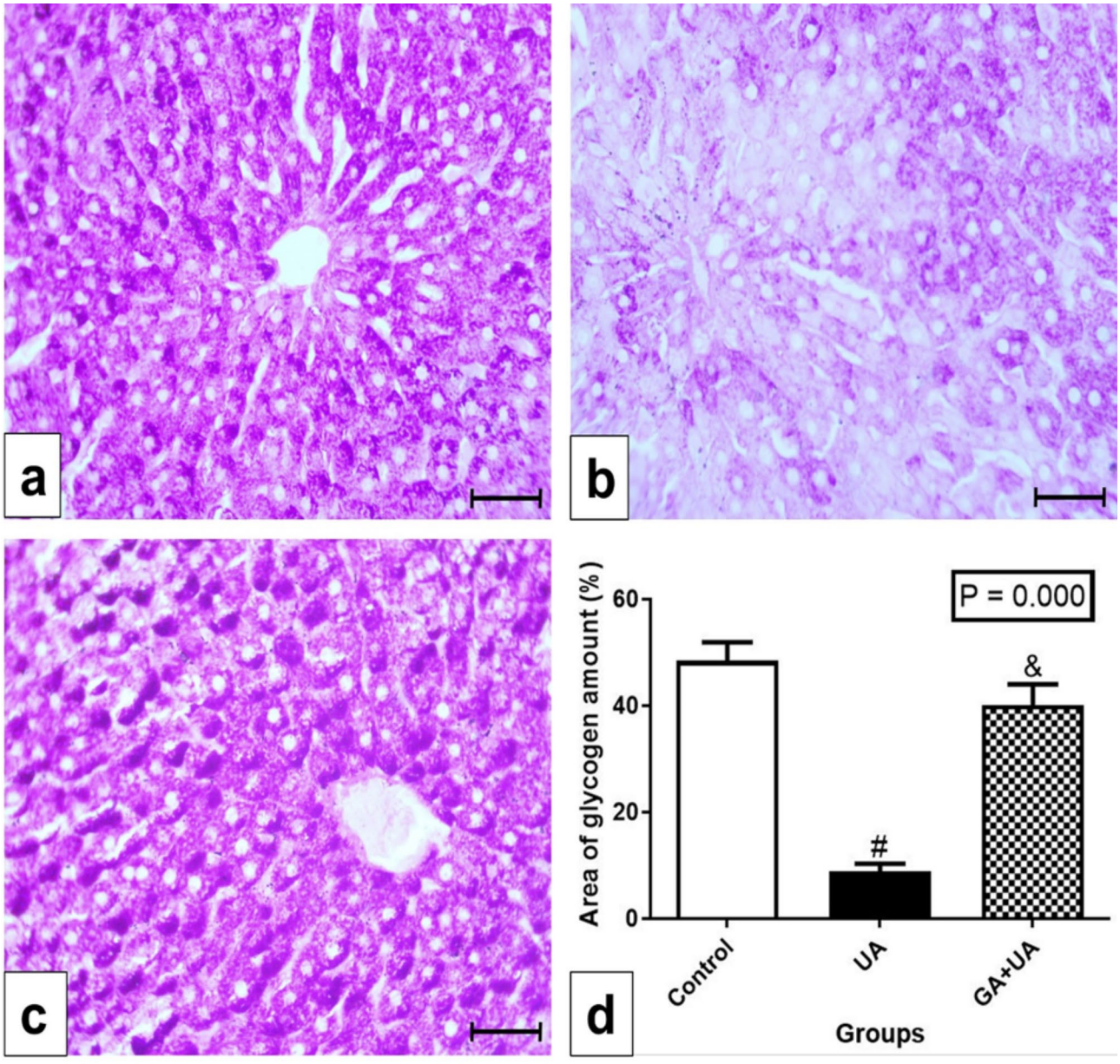

Fig. 5 Glycogen examination in the experimental groups. (**a**-**c**) photomicrographs of liver sections stained by Periodic acid–Schiff stain (PAS), bar = 50 µm. (**a**) In control group, showing great amount of glycogen represented as the positive reaction of PAS. (**b**) In UA group, showing noticeable depletion in glycogen content in most of the hepatocytes. (**c**) In GA + UA group, showing positive PAS reaction resembling those of control group. (**d**) Percentage of area of glycogen amount in the different experimental groups. Results are expressed as mean ± SEM of 3 rats per group (One-way ANOVA followed by Duncan post-test). # significant difference between UA and the control groups. & significant difference between GA + UA and UA groups

its reduced production due to extensive fibrosis [26, 39], resulting in an insignificant change in ALT and albumin following UA exposure.

Similar to gamma-irradiated rats [40], our experimental irradiated model displayed a marked increase in plasma glucose levels, attributed to mobilization of hepatic glycogen reserves as confirmed histologically. Reduced renal glucose excretion, decreased beta cell number, and impaired glucose uptake [41–43] contribute to this hyperglycemic state. Hyperglycemia-induced overproduction of reactive oxidants may disrupt endothelial tight junctions and the barrier function, leading to leakage of blood from vasculature into surrounding tissues [44]. UA-associated hyperglycemia appears to down-regulate gene expression of Nrf2 and its regulators [45]. Additionally, it down-regulates anti-apoptotic proteins, up-regulates pro-apoptotic factors, and promotes cytochrome c translocation from mitochondria to the cytosol [46]. In contrast, GA supplementation restored glucose homeostasis as demonstrated by Variya and colleagues

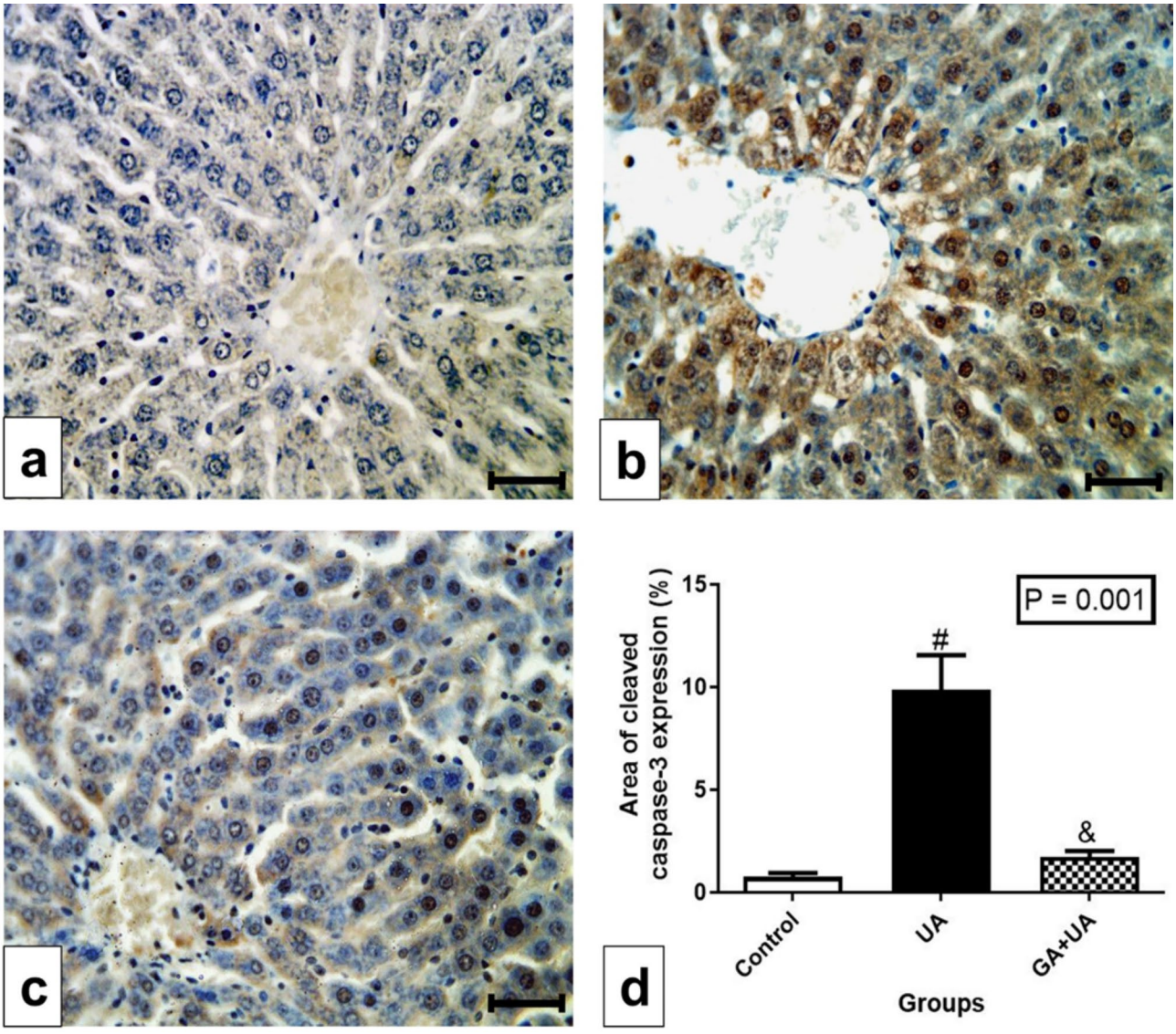

Fig. 6 Immunohistochemical detection of cleaved caspase-3 protein in the liver. (**a**-**c**) Photomicrographs of liver sections of rats from the experimental groups, bar = 50 µm. (**a**) In control group, showing negative immunoreaction for cleaved caspase-3. (**b**) In UA group, showing highly positive immunoreaction as represented by brown color specially in the nuclei of hepatocytes. (**c**) In GA + UA group, showing negative immunoreaction in most of the hepatocytes except few ones still with brown nuclei. (**d**) Percentage of area of cleaved caspase-3 protein expression in the different experimental groups. Results are expressed as mean ± SEM of 3 rats per group (One-way ANOVA followed by Duncan post-test). # significant difference between UA and the control groups & significant difference between GA + UA and UA groups

[47], achieved by delaying intestinal glucose absorption, enhancing beta-cell insulin secretion, and encouraging glucose uptake and peripheral insulin sensitivity [48].

The disturbances in lipid profile observed in the UA group are similar to the findings in gamma-irradiated rats [49]. Elevated activity of hepatic metabolizing enzymes responsible for fatty acid synthesis and mobilization contributes to radiation-induced hyperlipidemia [49]. Up-regulation in the transcript levels of sterol regulatory element-binding protein 1c might participate in this effect [50]. TG enrichment of HDL particles, enhancement of hepatic lipase activity, and inhibition of hepatic production of apolipoprotein A-1 may be responsible for the drop in plasma HDL-C [51]. Damage to the pancreas is a leading cause of inhibiting lipoprotein lipase [52], closely associated with the observed lipoprotein patterns [53]. A two-way relationship exists between hyperlipidemia and hyperglycemia. Hyperlipidemia promotes insulin resistance by blocking insulin signals and destroying pancreatic beta cells, giving rise to hyperglycemia [54]. As a consequence of excess glucose loading, lipid metabolism is impaired. For instance, glucose can be converted to fatty acids and cholesterol through *de novo* lipid biosynthesis pathways, and excessive lipids are

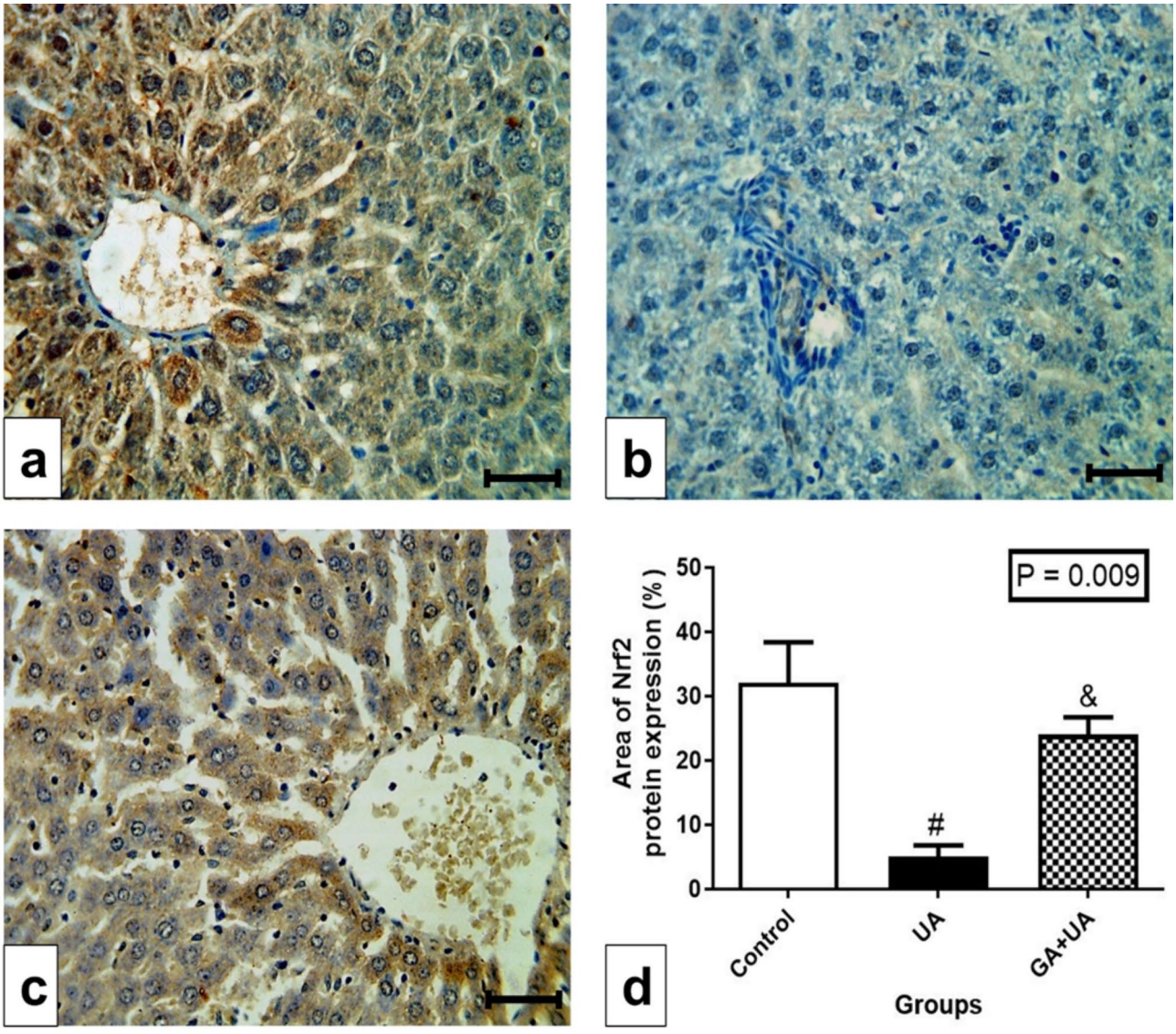

Fig. 7 Immunohistochemical detection of Nrf2 protein in the liver. (**a**-**c**) Photomicrographs of liver sections of rats from the experimental groups, bar = 50 µm. (**a**) In control group, showing positive immunoreaction of Nrf2 as represented by the brown color. (**b**) In UA group, showing negative immunoreaction (**c**) In GA + UA group, showing positive immunoreaction. (**d**) Percentage of area of Nrf2 protein expression in the different experimental groups. Results are expressed as mean ± SEM of 3 rats per group (One-way ANOVA followed by Duncan post-test). # significant difference between UA and the control groups. & significant difference between GA + UA and UA groups

secreted in lipoproteins or stored in lipid droplets [55]. Hyperglycemia can predispose to hypercholesterolemia by up-regulating 3-hydroxy-3-methylglutaryl-coenzyme A reductase, and hamper fecal cholesterol excretion and bile acid biomanufacturing [56, 57]. Peroxidation of membrane phospholipids exacerbates cholesterol biogenesis in the liver and other organs through overgeneration of peroxides and disruption of membrane structure-function attributes [58]. Hyperlipidemia induces hepatic oxidative stress, inflammation, and apoptosis [59]. The current GA intervention dosage and duration may be insufficient to counter UA-associated hyperlipidemia, as observed in atherosclerosis-prone apolipoprotein E knockout mice fed a high-fat Western-type diet [60]. Factors affecting gut microbial community and xenobiotic detoxification systems may play a dominant role in modulating the stability, absorption, and metabolism of phytochemicals [61].

The substantial increase in lipid peroxidation end products after UA intoxication concurs with findings by Yuan et al. [4]. UA stimulates excessive free radical production while inhibiting the intracellular redox stabilizing network in rat hepatocytes [62]. This impairment not only affects polyunsaturated fatty acids but can also impact other biological macromolecules, thereby affecting cellular membrane levels and subcellular components [63].

Our work, along with others [64], confirms the ability of GA to counteract the lipid peroxidation cascade in hepatic tissues due to its free radical scavenging properties. GA suppresses the Fenton reaction, which reduces the production of free radicals and the amount of iron available to combine with oxygen to initiate lipid peroxidation [65].

Matched with the depletion of NO in the testicular tissues of UA-exposed rats [8], our finding revealed a remarkable exhaustion of hepatic NO owing to a reduction in NO-secreting cells and inducible NO synthase activators and elevation in NO inhibitors [32]. Reduced NO bioavailability could result from its binding with superoxide radicals to form peroxynitrite or uncoupling of nitric oxide synthase under oxidative stress, further exacerbating the redox imbalance [66]. Disturbances in lipid metabolism in our irradiated model could contribute to NO depletion through mechanisms including L-arginine exhaustion (a key player in NO synthesis), NO synthase dysfunction, increased NO turnover, limited vascular response to its vasodilatory effects, and impaired translocation to target tissues [67]. The elevation in apoptotic signaling and reduction in cell proliferation capacity often correlate with a deficit in NO formation. This is evident from the cytoprotective properties of NO through S-nitrosylation of apoptotic mediators [68]. In contrast, GA supplementation increased hepatic NO levels, surpassing even control levels. This effect is due to the ability of GA to slow NO turnover and enhance endothelial NO synthase phosphorylation [69, 70]. Increased NO levels activate the pentose-phosphate pathway [71], a major NADPH producer that regenerates reduced GSH from its oxidized form. The elevation in NO levels correlates with the increase in SOD activity, suggesting a causal link. As SOD catalyzes the dismutation of superoxide radicals into molecular oxygen and hydrogen peroxide, heightened SOD activity clears superoxide anions, thus preserving NO bioavailability [72]. Additionally, NO is essential for up-regulating SOD expression, preventing superoxide radical-mediated NO degradation [73].

Similar to the findings of Hao et al. [74] and Pourahmad et al. [62], GSH redox network was altered in the UA group. This outcome indicates a failure in a critical component of the xenobiotic detoxification system [75], rendering the hepatic microenvironment more susceptible to the radiological hazards of UA. Lactic acidosis prompts metabolic reprogramming to enhance NADPH synthesis, shifting the glutathione redox couple towards the oxidized form to counter reactive oxidative stress [76]. Moreover, utilization of glutamine for ATP production under acidic stress contributes to the depletion of other glutamine-related metabolites, including GSH [76]. Reactive oxidant generation caused by UA triggers GSH oxidation and inactivation of GSH-related enzymes [77]. GST eliminates lipid peroxidation end-products and contaminants-derived electrophilic compounds [78, 79], thereby preventing cell membrane damage. The reduction in GST could be due to the down-regulation of its gene expression [80]. GSH is necessary for ensuring the continuation of thiol group reduction in mitochondrial membrane proteins [81]. When these thiol groups are oxidized, the pore complex undergoes structural modifications, resulting in a mitochondrial permeability transition that is a leading factor in both necrosis and apoptosis mechanisms [82]. Restoration of hepatic GSH redox cycle in the GA+UA group is compatible with what happened in doxorubicin-induced hepatotoxic [77] and streptozotocin-induced diabetic rats [65]. The increase in hepatic GSH levels in UA-irradiated rats pre-supplemented with GA is attributed to the up-regulation of gamma-glutamylcysteine synthetase, a rate-limiting enzyme in GSH biosynthesis [83]. Activation of Nrf2 results in increased transcript abundance of downstream antioxidants-related genes, including those belonging to the GSH redox system [84].

Total antioxidant capacity (TAC) provides a holistic view, accounting not only for the sum of individual antioxidants but also for their complex interactions [85]. The normalization of TAC reflects the ability of GA to restore the overall body's redox balance. The improved redox potency of hepatic tissue in the GA+UA group is attributed to increased transcript levels of antioxidants and scavenging of free radicals [86, 87]. This is supported by the increase in Nrf2 immuno-expression, a crucial transcription factor that plays a pivotal role in defending against peroxidative damage by up-regulating various enzymatic antioxidants. The Nrf2 signaling pathway is a critical mediator in controlling the transcription of numerous antioxidant genes, including enzymes involved in GSH and SOD synthesis [88]. GA disrupts the interaction between kelch-like ECH-associated protein 1 and Nrf2 in drug-induced hepatic dysfunction, leading to increased nuclear translocation of Nrf2 [83]. Sirtuin 1 overexpression resulting from GA supplementation facilitates Nrf2 nuclear translocation, stabilizes Nrf2 protein expression, and enhances nuclear accumulation, DNA binding activity and transcriptional function of Nrf2 [89, 90]. Targeting Nrf2 may offer a promising therapeutic strategy to enhance cellular stability against redox imbalances, a key factor in driving and exacerbating radiation-associated hepatic damage.

The hepatic histoarchitectural deteriorations induced by UA exposure are consistent with other reports [4, 91]. These cellular changes could arise from mitochondrial dysfunction and disruption of oxidative phosphorylation [1]. Vacuolated cytoplasm in the liver could result from dysregulated fatty acid metabolism, leading to neutral fat accumulation, which gets dissolved during tissue

preparation, leaving empty unstained vacuoles [92]. Karyolysis in hepatocytes, similar to uranium-contaminated mice [93], is attributed to endonuclease activity secreted by Kupffer cells, causing destructive fragmentation of genomic material [94]. The heightened release of reactive oxygen species, as indicated by increased MDA levels in the UA group, drives the excessive formation of extracellular matrix proteins ensuring optimum conditions for hepatic fibrosis [95]. Hyperlactemia resulting from increased LDH activity triggers transforming growth factor-beta, leading to fibroblast differentiation [96]. The marked occurrence of apoptotic hepatocytes following UA contamination aligns with findings in testicular germ cells [8]. UA triggers genotoxic damage indirectly through single-strand breaks, facilitated by oxidative DNA damage *via* Fenton redox reactions, and directly through covalent binding to DNA [97]. GA excretes antifibrotic activity by reducing hepatic pro-fibrogenic cytokines and blocking hepatic stellate cells activation and proliferation [98]. The anti-apoptotic effect of GA against UA-induced hepatotoxicity corresponds to its protection against ultraviolet radiation-induced damage in zebrafish and human keratinocytes [99]. Scavenging free radicals, reducing transcript levels of Bax and caspase-3, increasing Bcl-2 transcript levels, and enhancing genomic repair [9, 100] underlie the cytoprotective properties of GA.

Conclusion

Pre-treatment of UA-exposed rats with GA efficiently restored the liver's redox stability and cyto-functionality by inhibiting lipid peroxidation, up-regulating Nrf2, and suppressing the apoptotic cascade. This discovery holds significant value in guiding the scientific community toward recognizing the beneficial role of natural phytochemicals in mitigating the health risks associated with DU exposure. Further studies are highly recommended to highlight the molecular mechanisms underlying the protective effects of GA against UA intoxication.

Acknowledgements
We thank R.M. Mahfouz, Professor of inorganic chemistry, Department of Chemistry, Faculty of Science, Assuit University, Egypt, for their appreciable technical help.

Authors' contributions
NSA: designed the experiment, carried out the statistical analysis, and is the major contributor in writing the manuscript. HW: designed and carried out the experiment. AAIA performed the histological examination. SMMM carried out the experiment and performed the biochemical measurements. IMHE and EAN revised the draft. All authors have read and approved the final manuscript.

Funding
Not applicable.
Open access funding provided by The Science, Technology & Innovation Funding Authority (STDF) in cooperation with The Egyptian Knowledge Bank (EKB).

Data Availability
The datasets used and/or analyzed during the current study available from the corresponding author on reasonable request.

Declarations

Ethics approval and consent to participate
All procedures in this study adhered to the University guidelines for the care of experimental animals. Ethical approval (06/2023/0070) was obtained from the Research Ethics Committee of the Faculty of Veterinary Medicine, Assiut University, Egypt. The study is reported in accordance with ARRIVE guidelines.

Consent for publication
Not applicable.

Competing interests
The authors declare no competing interests.

Author details
[1]Department of Medical Physiology, Faculty of Medicine, Assiut University, Assiut 71526, Egypt
[2]Laboratory of Physiology, Department of Zoology and Entomology, Faculty of Science, Assiut University, Assiut, Egypt
[3]Department of Zoology and Entomology, Faculty of Science, Assiut University, Assiut, Egypt
[4]Department of Basic Medical Sciences, Faculty of Physical Therapy, Merit University, Sohag, Egypt
[5]Department of Physiology, Faculty of Veterinary Medicine, Assiut University, Assiut 71526, Egypt

Received: 13 May 2023 / Accepted: 8 November 2023
Published online: 22 November 2023

References

1. Yue YC, Li MH, Wang HB, Zhang BL, He W. The toxicological mechanisms and detoxification of depleted uranium exposure. Environ Health Prev Med. 2018;23:1–9.
2. Soltani M, Zarei MH, Salimi A, Pourahmad J. Mitochondrial protective and antioxidant agents protect toxicity induced by depleted uranium in isolated human lymphocytes. J Environ Radioact. 2019;203:112–6.
3. Shaki F, Hosseini MJ, Shahraki J, Ghazi-Khansari M, Pourahmad J. Toxicity of depleted uranium on isolated liver mitochondria: a revised mechanistic vision for justification of clinical complication of depleted uranium (DU) on liver. Toxicol Environ Chem. 2013;95:1221–34.
4. Yuan Y, Zheng J, Zhao T, Tang X, Hu N. Hydrogen sulfide alleviates uranium-induced acute hepatotoxicity in rats: role of antioxidant and antiapoptotic signaling. Environ Toxicol. 2017;32:581–93.
5. Yuan G, Dai S, Yin Z, Lu H, Jia R, Xu J, Song X, Li L, Shu Y, Zhao X. Sub-chronic lead and cadmium co-induce apoptosis protein expression in liver and kidney of rats. Int J Clin Exp Pathol. 2014;7:2905.
6. Šömen Joksić A, Katz SA. Chelation therapy for treatment of systemic intoxication with uranium: a review. J Environ Sci Health A Tox Hazard Subst Environ Eng. 2015;50:1479–88.
7. Ohmachi Y. Decorporation agents for internal radioactive contamination. J Pharm Soc Jpn. 2015;135:557–63.
8. Waly H, Ragab SMM, Hassanein KMA, Abou Khalil NS, Ahmed EA. Uranium exposure increases spermatocytes metaphase apoptosis in rats: inhibitory effect of thymoquinone and N-acetylcysteine. Gen Physiol Biophys. 2019;38:145–55.
9. Nair GG, Nair CKK. Radioprotective effects of gallic acid in mice. Biomed Res Int. 2013;2013:953079.
10. Ferk F, Chakraborty A, Jäger W, Kundi M, Bichler J, Mišík M, Wagner KH, Grasl-Kraupp B, Sagmeister S, Haidinger G, Hoelzl C, Nersesyan A, Dušinská M, Simić T, Knasmüller S. Potent protection of gallic acid against DNA oxidation: results of human and animal experiments. Mutat Res Fundam Mol Mech Mutagen. 2011;715:61–71.
11. Ma S, Lv L, Lu Q, Li Y, Zhang F, Lin M, Gao D, Liu L, Tian X, Yao J. Gallic acid attenuates dimethylnitrosamine-induced acute liver injury in mice through

Nrf2-mediated induction of heme oxygenase-1 and glutathione-s-transferase alpha 3. Med Chem. 2014;4:663–9.
12. Esmaeilzadeh M, Heidarian E, Shaghaghi M, Roshanmehr H, Najafi M, Moradi A, Nouri A. Gallic acid mitigates diclofenac-induced liver toxicity by modulating oxidative stress and suppressing IL-1β gene expression in male rats. Pharm Biol. 2020;58:590–6.
13. Friedewald WT, Levy RI, Fredrickson DS. Estimation of the concentration of low-density lipoprotein cholesterol in plasma, without use of the preparative ultracentrifuge. Clin Chem. 1972;18:499–502.
14. Saravanan R, Pari L. Effect of a novel insulinotropic agent, succinic acid monoethyl ester, on lipids and lipoproteins levels in rats with streptozotocin-nicotinamide-induced type 2 Diabetes. J Biosci. 2006;31:581–7.
15. Rojas MM, Villalpando DM, Ferrer M, Alexander-Aguilera A, García HS. Conjugated linoleic acid supplemented Diet influences serum markers in Orchidectomized Sprague-Dawley rats. Eur J Lipid Sci Technol. 2020;122:1900098.
16. Ohkawa H, Ohishi N, Yagi K. Assay for lipid peroxides in animal tissues by thiobarbituric acid reaction. Anal Biochem. 1979;95:351–8.
17. Ding AH, Nathan CF, Stuehr DJ. Release of reactive nitrogen intermediates and reactive oxygen intermediates from mouse peritoneal macrophages. Comparison of activating cytokines and evidence for Independent production. J Immunol. 1988;141:2407–12.
18. Misra HP, Fridovich I. The role of superoxide anion in the autoxidation of epinephrine and a simple assay for superoxide dismutase. J Biol Chem. 1972;247:3170–5.
19. Beutler E. Red cell metabolism. A manual of biochemical methods. 3rd ed. New York: Grune and Startton; 1984.
20. Tietze F. Enzymic method for quantitative determination of nanogram amounts of total and oxidized glutathione: applications to mammalian blood and other tissues. Anal Biochem. 1969;27:502–22.
21. Rotruck JT, Pope AL, Ganther HE, Swanson AB, Hafeman DG, Hoekstra WG. Selenium: biochemical role as a component of glutathione peroxidase. Science. 1973;179:588–90.
22. Habig WH, Pabst MJ, Jakoby WB. Glutathione S-transferases: the first enzymatic step in mercapturic acid formation. J Biol Chem. 1974;249:7130–9.
23. Bancroft JD, Gamble M. Theory and practice of histological techniques. 6th ed. Churchill Livingstone: Elsevier Health Sciences; 2008.
24. Bhutda S, Surve MV, Anil A, Kamath K, Singh N, Modi D, Banerjee A. Histochemical staining of collagen and identification of its subtypes by picrosirius red dye in mouse reproductive tissues. Bio-protocol. 2017;7:e2592.
25. Atia MM, Alghriany AA. Adipose-derived mesenchymal stem cells rescue rat hippocampal cells from aluminum oxide nanoparticle-induced apoptosis via regulation of P53, Aβ, SOX2, OCT4, and CYP2E1. Toxicol Rep. 2021;8:1156–68.
26. Ndrepepa G, Kastrati A. Alanine aminotransferase—a marker of cardiovascular risk at high and low activity levels. J Lab Precis Med. 2019;4:29–45.
27. Kimmoun A, Novy E, Auchet T, Ducrocq N, Levy B. Hemodynamic consequences of severe lactic acidosis in shock states: from bench to bedside. Crit Care. 2016;19:1–13.
28. Nouri A, Salehi-Vanani N, Heidarian E. Antioxidant, anti-inflammatory and protective potential of gallic acid against paraquat-induced liver toxicity in male rats. Avicenna J Phytomed. 2021;11:633–44.
29. Suwalsky M, Colina J, Gallardo MJ, Jemiola-Rzeminska M, Strzalka K, Manrique-Moreno M, Sepúlveda B. Antioxidant capacity of gallic acid in vitro assayed on human erythrocytes. J Membr Biol. 2016;249:769–79.
30. Panghal A, Sathua KB, Flora SJS. Gallic acid and MiADMSA reversed arsenic induced oxidative/nitrosative damage in rat red blood cells. Heliyon. 2020;6:e03431.
31. Nahar N, Mohamed S, Mustapha NM, Fong LS, Mohd Ishak NI. Gallic acid and myricetin-rich Labisia pumila extract mitigated multiple diabetic eye disorders in rats. J Food Biochem. 2021;45:e13948.
32. Hao Y, Ren J, Liu J, Yang Z, Liu C, Li R, Su Y. Immunological changes of chronic oral exposure to depleted uranium in mice. Toxicology. 2013;309:81–90.
33. Doi H, Hayashi E, Arai J, Tojo M, Morikawa K, Eguchi J, Ito T, Kanto T, Kaplan DE, Yoshida H. Enhanced B-cell differentiation driven by advanced Cirrhosis resulting in hyperglobulinemia. J Gastroenterol Hepatol. 2018;33:1667–76.
34. Tanaka S, Okamoto Y, Yamazaki M, Mitani N, Nakajima Y, Fukui H. Significance of hyperglobulinemia in severe chronic Liver Diseases–with special reference to the correlation between serum globulin/IgG level and ICG clearance. Hepatogastroenterology. 2007;54:2301–5.
35. Katz A, Orellana O. Protein synthesis and the stress response. In: Biyani M, editor. Cell-free protein synthesis. Crotia: Intech; 2012. pp. 111–34.
36. Zimmerman KL, Barber DS, Ehrich MF, Tobias L, Hancock S, Hinckley J, Binder EM, Jortner BS. Temporal clinical chemistry and microscopic renal effects following acute uranyl acetate exposure. Toxicol Pathol. 2007;35:1000–9.
37. Almalki DA, Alghamdi SA, Al-Attar AM. Comparative study on the influence of some medicinal plants on Diabetes induced by streptozotocin in male rats. Biomed Res Int. 2019;2019:3596287.
38. Wang G, Wang YF, Li JL, Peng RJ, Liang XY, Chen XD, Jiang GH, Shi JF, Si-Ma YH, Xu SQ. Mechanism of hyperproteinemia-induced blood cell homeostasis imbalance in an animal model. Zool Res. 2022;43:301–18.
39. Carvalho JR, Machado MV. New insights about albumin and Liver Disease. Ann Hepatol. 2018;17:547–60.
40. Ali MM, Ahmed OM, Nada AS, Abdel-Reheim ES, Amin NE. Possible protective effect of naringin (a citrus bioflavonoid) against kidney injury induced by?-irradiation and/or iron overload in male rats. Int J Radiat Res. 2020;18:673–84.
41. Hao Y, Huang J, Gu Y, Liu C, Li H, Liu J, Ren J, Yang Z, Peng S, Wang W. Metallothionein deficiency aggravates depleted uranium-induced nephrotoxicity. Toxicol Appl Pharmacol. 2015;287:306–15.
42. Mercantepe F, Tumkaya L, Mercantepe T, Rakici SY, Ciftel S, Ciftel S. Radioprotective effects of α2-adrenergic receptor agonist dexmedetomidine on X-ray irradiation-induced pancreatic islet cell damage. Naunyn Schmiedebergs Arch Pharmacol. 2023;396:1827–36.
43. Jo SK, Seol MA, Park HR, Jung U, Roh C. Ionising radiation triggers fat accumulation in white adipose tissue. Int J Radiat Biol. 2011;87:302–10.
44. Chen Y, Wang L, Pitzer AL, Li X, Li PL, Zhang Y. Contribution of redox-dependent activation of endothelial Nlrp3 inflammasomes to hyperglycemia-induced endothelial dysfunction. J Mol Med. 2016;94:1335–47.
45. Shivarudrappa AH, Ponesakki G. Lutein reverses hyperglycemia-mediated blockage of Nrf2 translocation by modulating the activation of intracellular protein kinases in retinal pigment epithelial (ARPE-19) cells. J Cell Commun Signal. 2020;14:207–21.
46. Parmar M, Syed S, Gray I, Ray JP. Curcumin, hesperidin, and rutin selectively interfere with apoptosis signaling and attenuate streptozotocin-induced oxidative stress-mediated hyperglycemia. Curr Neurovasc Res. 2015;12:363–74.
47. Variya BC, Bakrania AK, Patel SS. Antidiabetic potential of gallic acid from Emblica officinalis: improved glucose transporters and insulin sensitivity through PPAR-γ and Akt signaling. Phytomedicine. 2020;73:152906.
48. Abdel-Moneim A, Abd El-Twab SM, Yousef AI, Ashour MB, Reheim ESA, Hamed MAA. New insights into the in vitro, in situ and in vivo antihyperglycemic mechanisms of gallic acid and p-coumaric acid. Arch Physiol Biochem. 2022;128:1188–94.
49. Alkhalf MI, Khalifa FK. Blueberry extract attenuates γ-radiation-induced hepatocyte damage by modulating oxidative stress and suppressing NF-κB in male rats. Saudi J Biol Sci. 2018;25:1272–7.
50. Lestaevel P, Bensoussan H, Racine R, Airault F, Gourmelon P, Souidi M. Transcriptomic effects of depleted uranium on acetylcholine and cholesterol metabolisms in Alzheimer's Disease model. C R Biol. 2011;334:85–90.
51. Rashid S, Watanabe T, Sakaue T, Lewis GF. Mechanisms of HDL lowering in insulin resistant, hypertriglyceridemic states: the combined effect of HDL triglyceride enrichment and elevated hepatic lipase activity. Clin Biochem. 2003;36:421–9.
52. Razzaq DF, Saleh DS, Al-Mashhadani AH. Studying the uranium pollution in reduction the levels of the C-Peptide and Vitamin D for healthy and diabetic patients in Najaf City Iraq. AIP Conf Proc. 2020;2290:030038.
53. Hirano T. Abnormal lipoprotein metabolism in diabetic Nephropathy. Clin Exp Nephrol. 2014;18:206–9.
54. Zhou X, Zhang W, Liu X, Zhang W, Li Y. Interrelationship between Diabetes and periodontitis: role of hyperlipidemia. Arch Oral Biol. 2015;60:667–74.
55. Chen L, Chen XW, Huang X, Song BL, Wang Y, Wang Y. Regulation of glucose and lipid metabolism in health and Disease. Sci China Life Sci. 2019;62:1420–58.
56. Azizidoost S, Nazeri Z, Mohammadi A, Mohammadzadeh G, Cheraghzadeh M, Jafari A, Kheirollah A. Effect of hydroalcoholic ginger extract on brain HMG-CoA reductase and CYP46A1 levels in streptozotocin-induced diabetic rats. Avicenna J Med Biotechnol. 2019;11:234–8.
57. Li M, Zhou W, Dang Y, Li C, Ji G, Zhang L. Berberine compounds improves hyperglycemia via microbiome mediated colonic TGR5-GLP pathway in db/db mice. Biomed Pharmacother. 2020;132:110953.
58. Mansour HH, Ismael NER, Hafez HF. Modulatory effect of Moringa oleifera against gamma-radiation-induced oxidative stress in rats. Biomed Aging Pathol. 2014;4:265–72.
59. Paiva AA, Raposo HF, Wanschel ACBA, Nardelli TR, Oliveira HCF. Apolipoprotein CIII overexpression-induced hypertriglyceridemia increases nonalcoholic

fatty Liver Disease in association with inflammation and cell death. Oxid Med Cell Longev. 2017;2017:1838679.
60. Bai J, Lin QY, An X, Liu S, Wang Y, Xie Y, Liao J. Low-dose gallic acid administration does not improve diet-induced metabolic disorders and Atherosclerosis in apoe knockout mice. J Immunol Res. 2022;2022:7909971.
61. Redan BW, Buhman KK, Novotny JA, Ferruzzi MG. Altered transport and metabolism of phenolic compounds in obesity and Diabetes: implications for functional food development and assessment. Adv Nutr. 2016;7:1090–104.
62. Pourahmad J, Shaki F, Tanbakosazan F, Ghalandari R, Ettehadi HA, Dahaghin E. Protective effects of fungal β-(1→ 3)-D-glucan against oxidative stress cytotoxicity induced by depleted uranium in isolated rat hepatocytes. Hum Exp Toxicol. 2011;30:173–81.
63. Abou-Khalil NS, Ali MF, Ali MM, Ibrahim A. Surgical castration versus chemical castration in donkeys: response of stress, lipid profile and redox potential biomarkers. BMC Vet Res. 2020;16:1–10.
64. Ebaid H, Bashandy SA, Morsy FA, Al-Tamimi J, Hassan I, Alhazza IM. Protective effect of gallic acid against thioacetamide-induced metabolic dysfunction of lipids in hepatic and renal toxicity. J King Saud Univ Sci. 2023;35:102531.
65. de Oliveira LS, Thomé GR, Lopes TF, Reichert KP, de Oliveira JS, da Silva Pereira A, Baldissareli J, da Costa Krewer C, Morsch VM, Schetinger MRC. Effects of gallic acid on delta–aminolevulinic dehydratase activity and in the biochemical, histological and oxidative stress parameters in the liver and kidney of diabetic rats. Biomed Pharmacother. 2016;84:1291–9.
66. Guerby P, Tasta O, Swiader A, Pont F, Bujold E, Parant O, Vayssiere C, Salvayre R, Negre-Salvayre A. Role of oxidative stress in the dysfunction of the placental endothelial nitric oxide synthase in preeclampsia. Redox Biol. 2021;40:101861.
67. Laroia ST, Ganti AK, Laroia AT, Tendulkar KK. Endothelium and the lipid metabolism: the current understanding. Int J Cardiol. 2003;88:1–9.
68. Sun J, Morgan M, Shen RF, Steenbergen C, Murphy E. Preconditioning results in S-nitrosylation of proteins involved in regulation of mitochondrial energetics and calcium transport. Circ Res. 2007;101:1155–63.
69. Yan X, Zhang QY, Zhang YL, Han X, Guo SB, Li HH. Gallic acid attenuates angiotensin II-induced Hypertension and vascular dysfunction by inhibiting the degradation of endothelial nitric oxide synthase. Front Pharmacol. 2020;11:1121.
70. Kang N, Lee JH, Lee W, Ko JY, Kim EA, Kim JS, Heu MS, Kim GH, Jeon YJ. Gallic acid isolated from Spirogyra sp. improves Cardiovascular Disease through a vasorelaxant and antihypertensive effect. Environ Toxicol Pharmacol. 2015;39:764–72.
71. Iizumi T, Takahashi S, Mashima K, Minami K, Izawa Y, Abe T, Hishiki T, Suematsu M, Kajimura M, Suzuki N. A possible role of microglia-derived nitric oxide by lipopolysaccharide in activation of astroglial pentose-phosphate pathway via the Keap1/Nrf2 system. J Neuroinflammation. 2016;13:1–20.
72. Couto GK, Britto LRG, Mill JG, Rossoni LV. Enhanced nitric oxide bioavailability in coronary arteries prevents the onset of Heart Failure in rats with Myocardial Infarction. J Mol Cell Cardiol. 2015;86:110–20.
73. Bahnson ESM, Koo N, Cantu-Medellin N, Tsui AY, Havelka GE, Vercammen JM, Jiang Q, Kelley EE, Kibbe MR. Nitric oxide inhibits neointimal hyperplasia following vascular injury via differential, cell-specific modulation of SOD-1 in the arterial wall. Nitric Oxide. 2015;44:8–17.
74. Hao Y, Huang J, Liu C, Li H, Liu J, Zeng Y, Li R. Differential protein expression in metallothionein protection from depleted uranium-induced nephrotoxicity. Sci Rep. 2016;6:38942.
75. Shaw P, Chattopadhyay A. Nrf2–ARE signaling in cellular protection: mechanism of action and the regulatory mechanisms. J Cell Physiol. 2020;235:3119–30.
76. LaMonte G, Tang X, Chen JLY, Wu J, Ding CKC, Keenan MM, Sangokoya C, Kung HN, Ilkayeva O, Boros LG, Newgard GB, Chi JT. Acidosis induces reprogramming of cellular metabolism to mitigate oxidative stress. Cancer Metab. 2013;1:1–19.
77. Omobowale TO, Oyagbemi AA, Ajufo UE, Adejumobi OA, Ola-Davies OE, Adedapo AA, Yakubu MA. Ameliorative effect of gallic acid in doxorubicin-induced hepatotoxicity in Wistar rats through antioxidant defense system. J Diet Suppl. 2018;15:183–96.
78. Singhal SS, Singh SP, Singhal P, Horne D, Singhal J, Awasthi S. Antioxidant role of glutathione S-transferases: 4-Hydroxynonenal, a key molecule in stress-mediated signaling. Toxicol Appl Pharmacol. 2015;289:361–70.
79. Saadat M. An evidence for correlation between the glutathione S-transferase T1 (GSTT1) polymorphism and outcome of COVID-19. Clin Chim Acta. 2020;508:213–6.
80. Song Y, Salbu B, Teien HC, Evensen Ø, Lind OC, Rosseland BO, Tollefsen KE. Hepatic transcriptional responses in Atlantic salmon (Salmo salar) exposed to gamma radiation and depleted uranium singly and in combination. Sci Total Environ. 2016;562:270–9.
81. Zhang F, Xu Z, Gao J, Xu B, Deng Y. In vitro effect of manganese chloride exposure on energy metabolism and oxidative damage of mitochondria isolated from rat brain. Environ Toxicol Pharmacol. 2008;26:232–6.
82. Kowaltowski AJ, Netto LE, Vercesi AE. The thiol-specific antioxidant enzyme prevents mitochondrial permeability transition: evidence for the participation of reactive oxygen species in this mechanism. J Biol Chem. 1998;273:12766–9.
83. Feng RB, Wang Y, He C, Yang Y, Wan JB. Gallic acid, a natural polyphenol, protects against tert-butyl hydroperoxide-induced hepatotoxicity by activating ERK-Nrf2-Keap1-mediated antioxidative response. Food Chem Toxicol. 2018;119:479–88.
84. Sanjay S, Girish C, Toi PC, Bobby Z. Gallic acid attenuates isoniazid and rifampicin-induced liver injury by improving hepatic redox homeostasis through influence on Nrf2 and NF-κB signalling cascades in Wistar rats. J Pharm Pharmacol. 2021;73:473–86.
85. Silvestrini A, Meucci E, Ricerca BM, Mancini A. Total antioxidant capacity: biochemical aspects and clinical significance. Int J Mol Sci. 2023;24:10978.
86. Ojeaburu SI, Oriakhi K. Hepatoprotective, antioxidant and, anti-inflammatory potentials of gallic acid in carbon tetrachloride-induced hepatic damage in Wistar rats. Toxicol Rep. 2021;8:177–85.
87. Olayinka ET, Ore A, Ola OS, Adeyemo OA. Ameliorative effect of gallic acid on cyclophosphamide-induced oxidative injury and hepatic dysfunction in rats. Med Sci. 2015;3:78–92.
88. Li Z, Dong X, Liu H, Chen X, Shi H, Fan Y, Hou D, Zhang X. Astaxanthin protects ARPE-19 cells from oxidative stress via upregulation of Nrf2-regulated phase II enzymes through activation of PI3K/Akt. Mol Vis. 2013;19:1656–66.
89. Moghadam D, Zarei R, Vakili S, Ghojoghi R, Zarezade V, Veisi A, Sabaghan M, Azadbakht O, Behrouj H. The effect of natural polyphenols resveratrol, gallic acid, and kuromanin chloride on human telomerase reverse transcriptase (hTERT) expression in HepG2 hepatocellular carcinoma: role of SIRT1/Nrf2 signaling pathway and oxidative stress. Mol Biol Rep. 2023;50:77–84.
90. Zhang L, Chen Z, Gong W, Zou Y, Xu F, Chen L, Huang H. Paeonol ameliorates diabetic renal fibrosis through promoting the activation of the Nrf2/ARE pathway via up-regulating Sirt1. Front Pharmacol. 2018;9:512.
91. Sarhan HKA. Uranium and lead intoxication hazards induce hepatotoxicity in rats; biochemical, histochemical and histopathological studies. Egypt J Chem. 2021;64:4545–56.
92. Abd-Elkareem M, Abou Khalil NS, Sayed AH. Hepatotoxic responses of 4-nonylphenol on African catfish (Clarias gariepinus): antixoidant and histochemical biomarkers. Fish Physiol Biochem. 2018;44:969–81.
93. Guzmán L, Durán-Lara EF, Donoso W, Nachtigall FM, Santos LS. In vivo nanodetoxication for acute uranium exposure. Molecules. 2015;20:11017–33.
94. Takada S, Watanabe T, Mizuta R. DNase γ-dependent DNA fragmentation causes karyolysis in necrotic hepatocyte. J Vet Med Sci. 2020;82:23–6.
95. Ramos-Tovar E, Muriel P. Molecular mechanisms that link oxidative stress, inflammation, and fibrosis in the liver. Antioxidants. 2020;9:1279.
96. Kottmann RM, Kulkarni AA, Smolnycki KA, Lyda E, Dahanayake T, Salibi R, Honnons S, Jones C, Isern NG, Hu JZ, Nathan SD, Grant G, Phipps RP, Sime PJ. Lactic acid is elevated in Idiopathic Pulmonary Fibrosis and induces myofibroblast differentiation via pH-dependent activation of transforming growth factor-β. Am J Respir Crit Care Med. 2012;186:740–51.
97. Yellowhair M, Romanotto MR, Stearns DM, Lantz RC. Uranyl acetate induced DNA single strand breaks and AP sites in Chinese hamster ovary cells. Toxicol Appl Pharmacol. 2018;349:29–38.
98. El-Lakkany NM, El-Maadawy WH, El-Din SHS, Saleh S, Safar MM, Ezzat SM, Mohamed SH, Botros SS, Demerdash Z, Hammam OA. Antifibrotic effects of gallic acid on hepatic stellate cells: in vitro and in vivo mechanistic study. J Tradit Complement Med. 2019;9:45–53.
99. Wang L, Ryu B, Kim WS, Kim GH, Jeon YJ, Wang L, Ryu B, Kim WS, Kim GH, Jeon YJ. Protective effect of gallic acid derivatives from the freshwater green alga Spirogyra sp. against ultraviolet B-induced apoptosis through reactive oxygen species clearance in human keratinocytes and zebrafish. Algae. 2017;32:379–88.

100. Zhou D, Yang Q, Tian T, Chang Y, Li Y, Duan LR, Li H, Wang SW. Gastroprotective effect of gallic acid against ethanol-induced gastric Ulcer in rats: involvement of the Nrf2/HO-1 signaling and anti-apoptosis role. Biomed Pharmacother. 2020;126:110075.

Publisher's Note